



Interfacial processes during diffusion welding of titanium alloy/aluminium couples under ambient atmosphere

M. Kamal Karfoul¹ · Gordon J. Tatlock²

Received: 1 May 2018 / Accepted: 2 February 2019 / Published online: 13 February 2019
© International Institute of Welding 2019

Abstract

In this study, it is reported that the diffusion welding of α -titanium and ($\alpha + \beta$) titanium alloys with aluminium has been carried out by applying sufficient compression to the welded samples to give a high level of plastic deformation in the Al layers sandwiched between layers of titanium alloy with a moderate surface finish. Both metals are active in the air; such diffusion processes can take place under vacuum. However, we report, that high-quality welds were achieved at temperatures between 610 and 630 °C under ambient air atmosphere, without the use of vacuum or reducing atmospheres. The resulting microstructures and intermetallic phases were characterised using scanning and transmission electron microscopy and EDX microanalysis. This showed that under the welding parameters selected, Ti diffused across the interface into Al and Al into Ti, since the protective Al₂O₃ thin film on the surface of aluminium layer has been disrupted due to the Al layer plastic deformation. Impact tests of welds gave relatively high energy impact values.

Keywords Diffusion welding · Ti alloys · Al alloys · Microstructures · Interface · Intermetallics

1 Introduction

Titanium (Ti) is a key metal in a wide spectrum of industry. The question of welding Ti and its alloys has become very important, and at the present time Ti welding to aluminium (Al) has gained widespread use in the aerospace and automobile industries. However, the fusion welding of these dissimilar metals has several problems such as the formation of brittle intermetallic phases at the welded interface. Mostly to avoid the influence of environmental air, the welding areas have to be protected by a special inert gas. Some applications use a dissimilar metal interlayer between the welded base metals and may thus be helpful. Majumdar et al. [1] carried out continuous CO₂ laser welding of Ti6Al4V alloy to

wrought aluminium using Nb foil, which was added as a buffer between the Ti alloy and Al alloy workpieces. Oliveira et al. [2] achieved pulse laser welding of memory alloy NiTi to TiAl6V using a Nb-interlayer. The authors of these works reported that the Nb-layer acted as a diffusion barrier which prevented the formation of brittle intermetallic phases at the interface as the Nb layer did not melt completely. It is well known [3] that Ti from the structure of Ti alloys completely dissolves in Nb on both sides of the interlayer, while Al with Nb forms an intermetallic compound NbAl₃. This phase was noticed in the Al side close to Nb/Al interface [1]. It is brittle and may cause cracks at the interface.

Similarly, for welding of Ti-alloy with aluminium solid-state welding seems to be the best choice. Explosive welding in the metallurgical industry has wide application for the production of double Ti-Al sheets. But in common welding practice, such methods cannot be used to weld several kinds of Ti alloys with Al substrates. In these cases, diffusion welding will be preferable, as it can be carried out at temperatures below the Al melting point and does not reduce the properties of the Ti substrate. However, the widespread use of diffusion welding (DW) of titanium to aluminium is slowed down by problems concerning cracking associated with the formation of brittle intermetallic phases at the Ti/Al interface. Both Ti and Al are active metals. At room temperature, they react with

Recommended for publication by Commission XVII - Brazing, Soldering and Diffusion Bonding

✉ M. Kamal Karfoul
karfoulmk@yahoo.co.uk

¹ Faculty of Mechanical & Electrical Engineering, Al-Baath University, Homs, Syria

² Department of Mechanical, Materials and Aerospace Engineering, School of Engineering, The University of Liverpool, The Quadrangle, Brownlow Hill, Liverpool L69 3GH, UK

the oxygen in the air forming surface oxides which can inhibit interdiffusion, therefore, the welding is carried out in vacuum.

To date, there has been only a small amount of information about the diffusion welding of Ti with Al. Enjyo et al. [4, 5] studied DW at temperatures between 600 and 660 °C in vacuum. The authors stated that welded samples were brittle and cracked under tensile test on the Al side of the interface. Another study [6] showed diffusion bonding of multi-laminated Ti/Al foils. The samples were preliminary cold rolled to obtain 56% reduction in thickness. Then, the compressed samples were diffusion welded at 660–680 °C. The authors noted that an intermetallic phase—a TiAl₃ layer—was formed at the Ti/Al interface and that Ti diffused into Al, but the Al did not diffuse into Ti. Other authors [7] reported that after an annealing time of about 150 h a brittle phase of TiAl₃ was formed, which was supposed to be the reason for specimen cracking. The authors also indicated diffusion of both Al and Ti into one another. However, it is clear that the diffusion time here is not suitable for a welding process. In another study [8], the authors suggest separation the joining process into four stages, as there is a delay before TiAl₃ is generated. It has been shown that high levels of plastic deformation give an improved weld [9, 10]. In any case, during the welding process, Al and Ti oxides should not remain at the Ti/Al interface as continuous films. Compression during welding probably has a positive effect on diffusion process by dispersing the Al oxide film, which may be further disrupted if plastic deformation is used. Ti oxide may also be reduced by Al. Hence, further analysis at high resolution could give new insight into the process, which could be of real importance if DW under ambient atmosphere can be routinely achieved. This article is devoted to an investigation of the interfacial diffusion processes that occur, when Ti/Al composites are subjected to diffusion welding under ambient atmosphere.

2 Experimental procedure

For welding experiments, metallic thin plates of Ti-5Al (designated as Ti), Ti-6Al-4 V (TiV) and Al 1100 (Al) were used. Metal composition and dimensions for experimental sample groups are listed in Table 1. Ti and TiV plates were roughened with silicon carbide paper No 600 washed with detergent and water, and before being assembled with pieces of aluminium in the form of a sandwich all plates were kept under ethanol to

Table 1 Metallic plates characteristics

Metal	Symbol	Dimensions, mm
Ti-5Al	Ti	0.6 × 9 × 55
Ti-6Al-4 V	TiV	0.8 × 9 × 55
Al 1100	Al	0.4 × 9 × 55

be sure that no surface contaminations remained. Fifty micrometres tungsten wires were placed between metallic layers as neutral markers in order to monitor the diffusion processes at the interface (Fig. 1). The sandwich sample was then carefully inserted into a special test rig with maximum load capacity of about 100 kN. The sample was compressed to 50% of max load while the W-wires remained at the interface between Ti and Al. The samples were then heated to 500 °C with an electric heater in air. At this temperature, the pressure was increased to 100% of the maximum load, whereupon, the sandwiches were heated to different welding temperatures as shown in the matrix, (Fig. 2a).

Samples for further investigation on light, scanning (SEM), and transmission (TEM) electron microscopy were taken from the cross section of welded sandwiches. The SEM used was a JEOL JSM 35 C at a voltage 30 kV. The TEM was a JEOL-2000 FX II at 200 kV.

Specimens for TEM studies were cut into thin slices about 8 × 6 × 0.25 mm. A low speed diamond saw was used for slicing. These slices were mechanically thinned and polished to a thickness of 30–50 μm. Single hole 2000 μm support copper rings were then glued to the surfaces of the slices on both sides, so that at least one of the sandwich interfaces will be at the centre of the ring. Then, the TEM specimens in disc form were carefully cut out. Then the specimens were thinned by conventional argon ion beam milling in a precision ion polishing system (PIPS) until holes appeared at or near the Ti/Al interface. The holes forming were observed periodically with an optical microscope. EDX analyses were carried out in the TEM.

All welded samples were exposed to V-notch impact Charpy tests in the transverse direction, as described in the ASTM E 23–07a conditions for non-standard specimens on a Charpy pendulum test machine. For the impact test, 3 specimens were used at each holding time and temperature level (Fig. 2b). Welded specimens for the study were selected by visual control and impact testing results. The samples observed with cracks or fractures during the whole welding period, including the mechanical finishing afterwards, were considered as being unsuccessfully welded. Experimental results

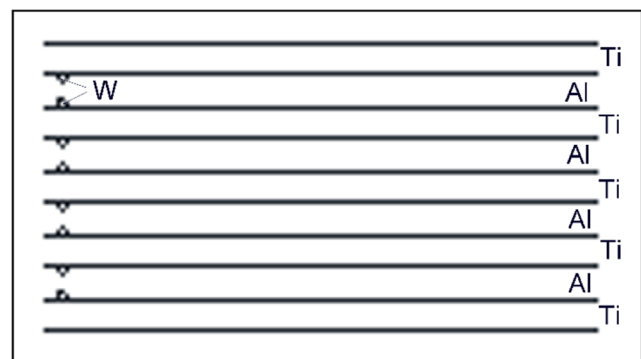


Fig. 1 Sandwich plates assembling scheme

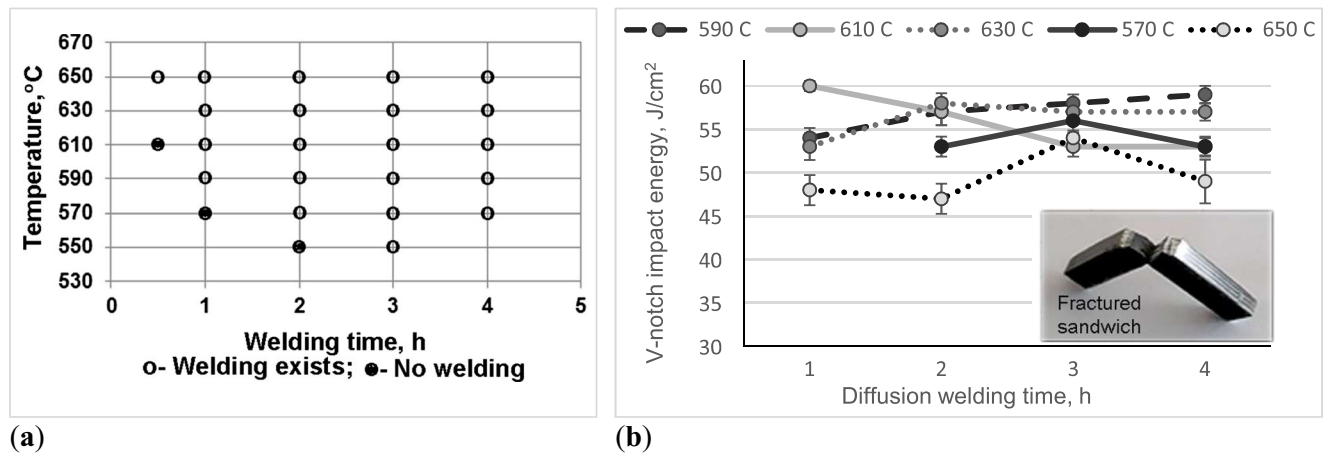


Fig. 2 Arranged Ti/Al welding experiments: (a) experiments matrix data; (b) impact absorbed energy of welded sandwiches Ti/Al

are presented graphically in Fig. 2b with error bars indicating the standard error.

3 Experimental results

Two series of experiments were performed, Exp A and Exp B. For Exp A, Ti/Al diffusion welding was attempted over the temperature range between 550 and 650 °C in ambient air atmosphere according to the matrix shown in Fig. 2a. Figure 3 shows cross sections of welded sandwiches. In Fig. 3a, it can be clearly observed that the interface has moved from the W-markers to within the Ti layer. This indicates the ongoing diffusion at the Ti/Al interface. The thickness of the sandwiches was reduced by 5–14% during the welding process.

The values of the impact absorbed energy were close to those of diffusion welded Ti/Ti joints [11]. The welded sandwiches having the best toughness (Fig. 2b, point 610 °C, 60 Jcm⁻², 1 h) were selected for further research. In order to compare the DW of α -Ti (Ti-5Al) to Al (Exp A), with ($\alpha + \beta$) Ti alloy (Ti-6Al-4 V) to Al (Exp B) the parameters given in Table 2 were used.

Light microscopy and SEM (Fig. 3a, b), as well as TEM images (Fig. 4) showed that the DW processes were carried out successfully, and that the weldments were defect-free. The Ti-alloy/Al interface zone had a thickness of 0.1 μ m on the Ti alloy side and about 0.4 μ m on the Al side of the interface (Fig. 4a).

Diffraction patterns were recorded from positions close to the diffusion zones at the interface (Fig. 5). The area on the Ti alloy side has a hexagonal Ti lattice (hcp) structure with a zone axis shown in Fig. 5a. On the Al side the metal has a face centred cubic (fcc) lattice with a [212] zone axis shown in Fig. 5b. EDX analyses from positions on both sides of the (Ti alloy)/Al interface confirm that Al had diffused across the interface into the Ti-rich layer and Ti had diffused into the Al-layer. EDX results are recorded in Table 3 and Fig. 6a, b.

4 Discussion

4.1 Diffusion processes at the interface

Tracing the Ti and Al concentrations in the diffusion field closed to the interface for Exp.A, we can identify four zones (Fig. 6a). On the Ti side, close to the interface, zone 1 contains the Ti₃Al and TiAl phases. At a distance of 100 nm from the interface, the Al concentration decreases to 28 at.% with a corresponding Ti concentration, $C_1 = 72$ at.% which may correspond to a Ti₃Al phase. At a distance of 500 nm from the original interface the Al concentration decreases to 8 at.% ($Ti - C'_1 = 92$ at.%) as zone 2 is entered. It then drops smoothly to the initial Al concentration of 5 at. % ($Ti - C_{0T} = 95$ at.%). At the other edge of zone 1, at the interface, the Ti content was measured as $C_S = 45$ at. %, (Al = 55 at.%) which may correspond to a TiAl phase. The titanium concentration then falls sharply to 28 at. % (Al = 72 at.%) as zone 3 is entered. Here, it is probably that another intermetallic phase such as TiAl₃ and/or TiAl₂, has formed since, thermodynamically, these phases are the most stable when the Ti concentration is between 25 and 33 at.%, (Al-Ti phase diagram [3]). The results of EDX analyses in regions 100–400 nm from the original interface into the Al layer show a Ti content $C_2 = 27$ at. % corresponding to a TiAl₃ phase. In fact, this band continues out beyond 400 nm, until zone 4 is entered at a distance of about 500 nm. Here, the Ti content drops to 8 at.%. Further EDX analysis shows a smoothly decreasing Ti content to its initial value in Al ($C_{0A} = 0\%$) at a distance of about 1.5 μ m from the original interface.

For Exp B, (Table 3 and Fig. 6b), we have similar to Exp A results, but with some changes in elemental values and different phases present, since the diffusion rate has changed due to the presence of vanadium in the double ($\alpha + \beta$) Ti alloy composition. To simplify the calculation, since the atomic radii of Ti and V are close, we treated the influence of vanadium as being similar to that of Ti, thus putting the sum of (Ti + V) rather than Ti when plotting the variation in concentration across the diffusion couples.

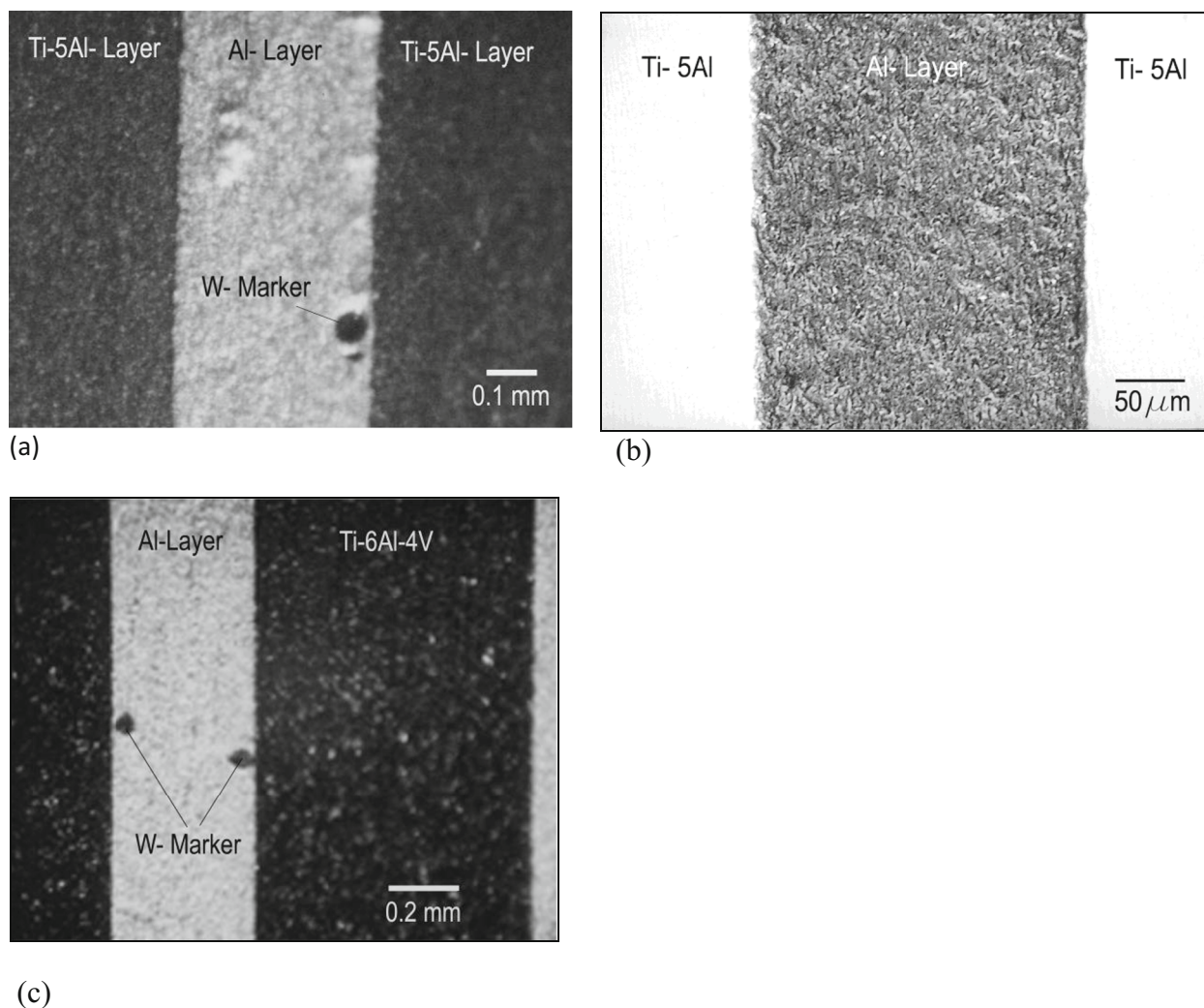


Fig. 3 Images of sandwich cross sections after welding: **(a)** Ti-5Al alloy light microscopy image (610 °C, 1 h); **(b)** Ti-5Al alloy SEM image (650 °C, 1 h); **(c)** Ti-6Al-4 V alloy light microscopy image (630 °C, 3 h)

Use of the TEM for the investigation of the Ti/Al diffusion process for reasonable diffusion welding times revealed Al diffusion into Ti alloy, as well as Ti diffusion into Al. Therefore, to model this complex system, simultaneous Al and Ti diffusion in both Ti- and Al-rich regions should be taken in consideration. These diffusion processes may lead to the formation of intermetallic phases on the both sides of the original interface. Each of these phases has its own boundary plane. So, the Ti- and Al-rich regions of diffusion system can be divided in two zones (Fig. 6c).

In the Ti-rich region, the first zone relates to the space between the interface and the boundary plane of the Ti_3Al

intermetallic phase, with Al diffusion coefficient D_1 . The second zone is the remaining part of the Ti-rich area with Al diffusion coefficient in Ti, D_2 . The ratio of these coefficients D_1/D_2 equals φ_1 . In Al-rich region the two zones have diffusion coefficients assigned: D_3 -titanium diffusion coefficient in $TiAl_3$ rich phase zone 3, D_4 -titanium diffusion coefficient in the Al-Ti alloy zone 4, with $D_3/D_4 = \varphi_2$. If one of diffusion coefficients in the zone is known, the other can be determined. The model of Ti and Al diffusion process may be described by the changing the positions of the Ti_3Al and $TiAl_3$ phase planes with time (t).

To derive the diffusion coefficients, a model of the diffusion process based on the tabulated data for the main system components at the interface and adjacent fields can be represented as function of the concentration values and the diffusion depth $c = f(x)$, (Fig. 6).

Thus, the Al atomic fraction in Ti part (c) at distances from the interface (x) has the values corresponding to Ti_3Al -rich phase zone. For diffusion time $t > 0$, co-ordinate $x = \xi_1$

Table 2 Diffusion welding parameters

Samples groups	Heating temperature, T °C	Heating time, t, h
Exp.A (Ti + Al)	610	1
Exp.B(TiV + Al)	630	3

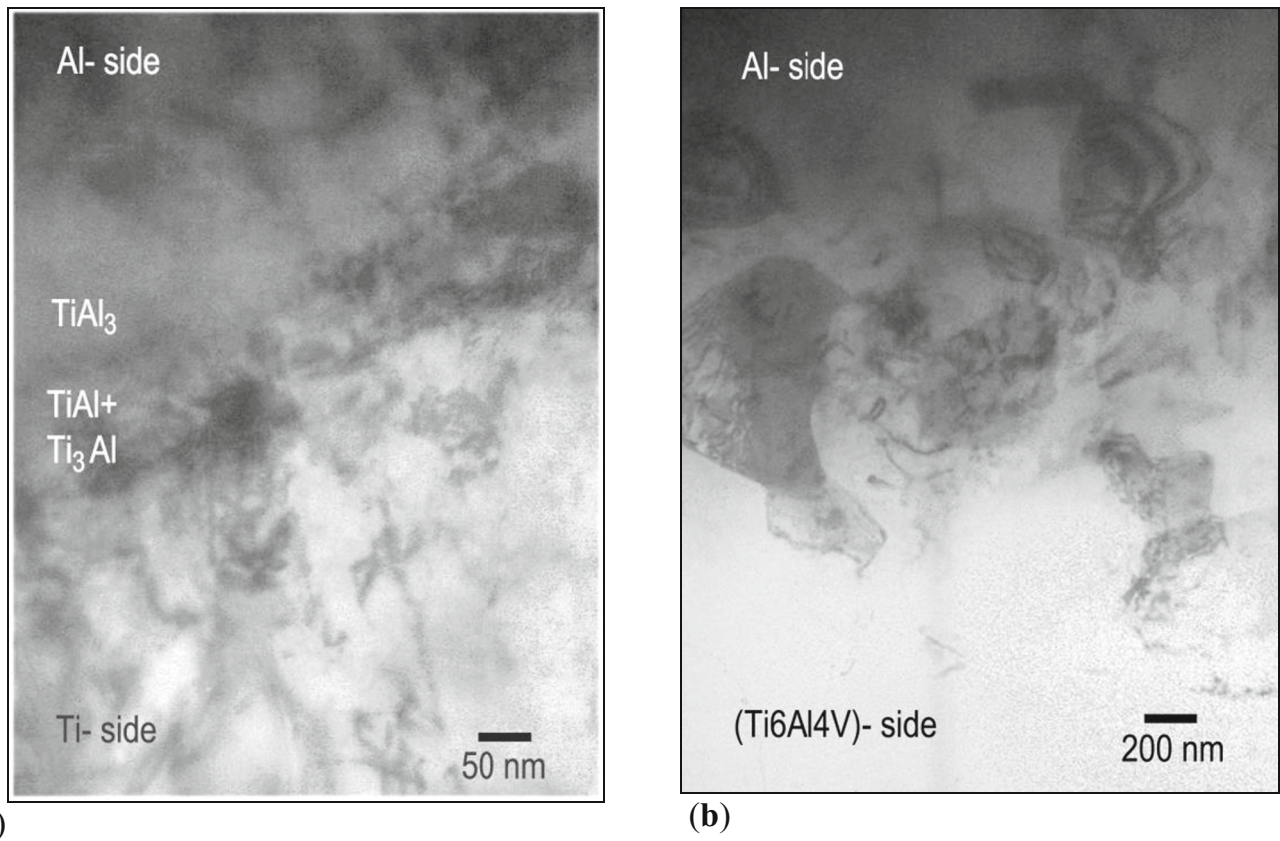


Fig. 4 TEM images at the original interfaces: **(a)** Ti/Al ($T=610\text{ }^{\circ}\text{C}$, $t=1\text{ h}$); **(b)** TiV/Al ($T=630\text{ }^{\circ}\text{C}$, $t=3\text{ h}$)

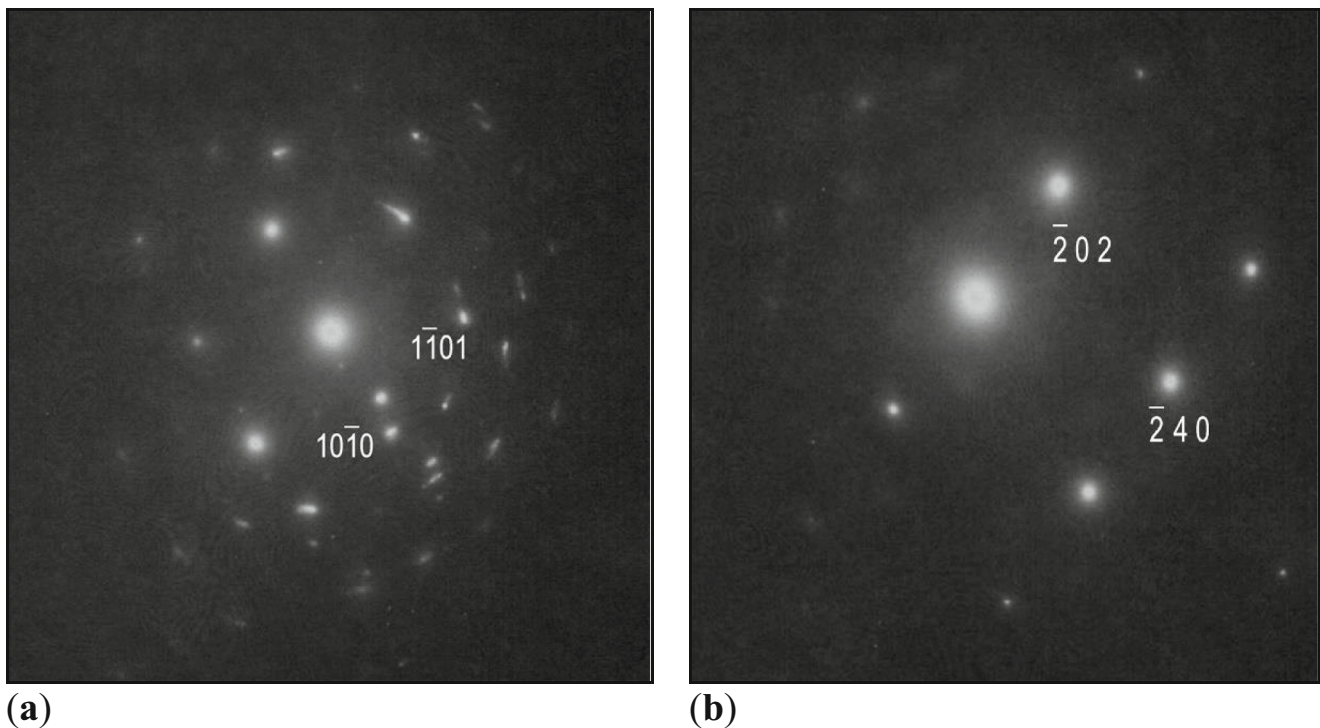


Fig. 5 Diffraction patterns on spots near the interface: **(a)** on spot at 500 nm on Ti side, zone axis $[\bar{1}2\bar{1}3]$; **(b)** on spot at 500 nm on Al side, zone axis $[212]$

Table 3 EDX analyses results in diffusion systems A and B

Interface side	Distances from interface, nm	Ti and Al concentrations			
		Exp A, at. %	Symbol (phase)	Exp B, at. %	Symbol (phase)
Ti-alloy	-1500	Al = 5, Ti = 95	C_{0T} (Ti)	Al = 4.8, Ti = 90, V = 5	C_{0T} (TiV)
	-500	Al = 8, Ti = 92	C'_1 (Ti)	Al = 5, Ti = 89, V = 5	C'_1 (TiV)
	-300	–	–	Al = 27, Ti = 67, V = 5	C_1 (Ti ₃ Al)
	-100	Al = 28, Ti = 72	C_1 (Ti ₃ Al)	Al = 40, Ti = 54, V = 5	C_S (TiAl)
Al	+0.00	Al = 55, Ti = 45	C_S (TiAl)	–	–
	+100	Al = 72, Ti = 28	C_2 (TiAl ₃)	Al = 58, Ti = 39, V ≈ 3	(TiAl)
	+200	–	–	Al = 79, Ti = 18, V = 2.6	C_2 (Ti Al ₃)
	+400	Al = 73, Ti = 27	C_2 (TiAl ₃)	Al = 94, Ti ≈ 5.6, V < 0.1	C_3 (Al-Ti)
	+500	Al = 92, Ti = 8	C_3 (Al-Ti)	Al = 94, Ti ≈ 5.6, V < 0.1	(Al-Ti)
	+1000	Al = 95, Ti = 5	–	–	–
	+1500	Al = 99, Ti = 1	–	Al = 96, Ti ≈ 3.6	(Al-Ti)
	+2000	Al = 99, Ti < 1	C_{0A} (Al)	–	–
	+5000	–	–	Al = 98, Ti < 1	C_{0A} (Al)

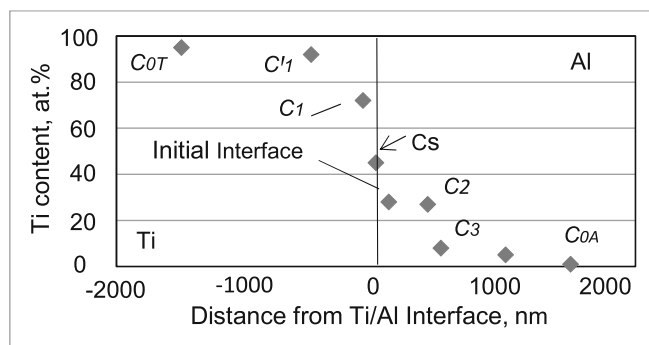
corresponds to the boundary Ti₃Al phase plane position. In accordance with Seith [12] and Reed-Hill [13] interpretations the Fick’s first diffusion law will take the form:

$$\xi_1 = 2b_1\sqrt{D_1t} \tag{1}$$

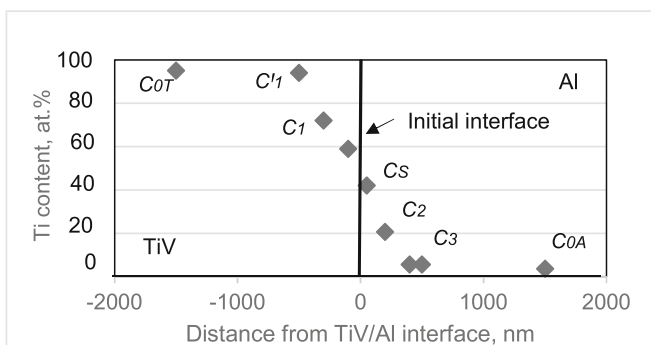
where b_1 is dimensionless constant for zone 1.

For initial conditions $t = 0, c = C_{0T} = 5$ at. % (Ti = 95 at. %), and boundary conditions (for zone 1): $x = \xi_1, c = C_1$, and $x = 0, c = C_S$, the mass balance equation at the boundary of the Ti₃Al phase plane leads to the expression:

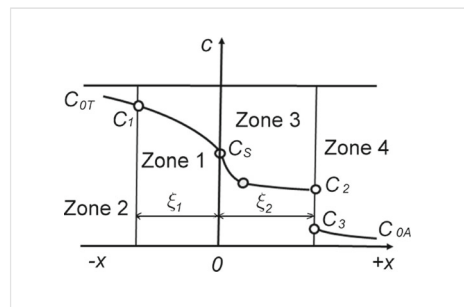
$$(C_1 - C'_1) \frac{d\xi_1}{dt} = -D_1 \left(\frac{\partial c}{\partial x} \right)_{C_1} + D_2 \left(\frac{\partial c}{\partial x} \right)_{C'_1} \tag{2}$$



(a)



(b)



(c)

Fig. 6 Ti concentration function of diffusion deepness, $c = f(x)$: (a) Exp A; (b) Exp B; (c) Scheme of diffusion system zones

In the Al-rich region, the space between the interface position ($x = 0$) and TiAl_3 intermetallic phase has a thickness ξ_2 in zone 3, while the Ti atoms which penetrate across the boundary of the TiAl_3 phase form an Al-Ti alloy in zone 4. As well as for zone 1, by means of parabolic law for diffusion layer growth [12, 13] the expression describing Ti mass flow across boundary plane $x = \xi_2$ is represented as follows:

$$\xi_2 = 2b_3\sqrt{D_3t} \quad (3)$$

where b_3 is dimensionless constant for zone 3.

For initial condition $t = 0$, $c = C_{0A} = 0$, and boundary conditions for TiAl_3 phase (zone 3): at $x = 0$, $c = C_S$ and at $x = \xi_2$, $c = C_2$; and for the space of zone 4: at $x = \xi_2$, $c = C_3$ and at $x = \infty$, $c = C_{0A}$, the mass balance equation at the boundary between zone 3 and zone 4 takes the following form:

$$(C_2 - C_3) \frac{d\xi_2}{dt} = -D_3 \left(\frac{\partial c}{\partial x} \right)_{C_2} + D_4 \left(\frac{\partial c}{\partial x} \right)_{C_3} \quad (4)$$

The method of Seith [12] based on Fick's second law and the Kirkendall effect can be applied for calculation of parameters for the diffusion processes multiphase solid system for time $t > 0$. The calculated parameters for the diffusion processes in zones 1/2 and 3/4 are illustrated in Table 4.

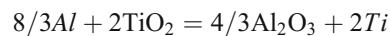
It is necessary to note, that the Ti diffusion rate in Al-rich region for Exp.A is 10 times greater than for Exp.B. It is likely that the presence of V in the TiV alloy inhibits the movement of Ti within the Al rich layer. For the Ti-rich region, the diffusion coefficients in zones 1 and 2 are the same. This explains why there is no sharp concentration drop at the Ti_3Al boundary plane. Basing on the calculation model that led to Table 4 data, we can select the optimal parameters for Ti diffusion welding to Al. The conditions for successful welding should minimise the diffusion time and temperature, since the TiAl_3 phase formed at the interface region should have a minimum thickness.

4.2 Destruction of oxide films on the surfaces of Al and Ti alloy at the interface

Under ambient air conditions, the aluminium surface is always covered by a thin Al-oxide layer. This oxide is thermodynamically stable and protects the metallic aluminium substrate from further reaction with air. Any Ti diffusing during the welding process at temperatures less than the melting point of Al has to cross the Ti/Al interface, which contains an Al-

oxide film. This film is compact, so in principle Ti diffusion should be extremely difficult. However, Ti and Al diffusion across Ti/Al interface has been observed. Hence presumably, the Al oxide film has been disrupted. The breakup of the protective Al_2O_3 scale on the aluminium layer may be promoted by the roughness of the Ti surfaces [10]. According to the authors of this paper, the applied pressure causes a high level of plastic deformation of the Al. The Al-oxide film conforms to the Ti surface morphology at the Ti/Al interface and the oxide cracks [10, 14–16]. Hence, to promote cracking, the critical roughness value Rz for buckling needs to be exceeded. At 610 °C for a growth time of 1 h, the oxide thickness is about 19.6 nm [17]. Thus, the calculated Rz required to give decohesion is 0.16 μm , which is likely to be exceeded unless the Ti is polished or ground very finely. The dispersion of the oxide layer speeds up the Ti diffusion across the Ti/Al interface, and fragments of Al oxide may be observed in Fig. 4. This is consistent with the oxygen signals present in the spectra shown in Fig. 7b, and clear evidence of the penetration of Ti between the pieces of Al oxide film at the interface is presented in Fig. 7a.

On the other hand, the Ti surface is normally covered by a thin, protective film of Ti-oxide. This oxide film is not completely stable at welding temperatures of 610–630 °C. It starts to dissociate near these temperatures, and the released oxygen dissolves in the Ti [18, 19]. Also, due to the big difference in the free energy of formation of Ti and Al oxides [17], the reaction:



between TiO_2 and Al (after the cracking of the Al oxide scale) is thermodynamically enabled.

Thus Ti-oxide collapses, and the diffusion of Ti across the interface becomes possible. Since the oxide films are destroyed, the welding process can proceed, and the properties of the welded joint under ambient atmosphere will be similar to that under vacuum atmosphere.

5 Conclusions

1. In this study, the diffusion welding of multi-laminated sandwiches of Al layers between Ti alloy layers with a moderate surface finish was carried out at temperatures below the melting point of Al in ambient air atmosphere. The critical step was the plastic deformation of Al layers

Table 4 The calculated parameters for diffusion processes in zones 1/2 and 3/4

Experiment	b_1	b_3	φ_1	φ_2	ξ_1 , nm	ξ_2 , nm	D_1 , $\text{cm}^2 \text{s}^{-1}$	D_2 , $\text{cm}^2 \text{s}^{-1}$	D_3 , $\text{cm}^2 \text{s}^{-1}$	D_4 , $\text{cm}^2 \text{s}^{-1}$
Exp.A	0.69	0.60	1	4	100	400	1.5×10^{-14}	1.5×10^{-14}	3×10^{-13}	0.77×10^{-13}
Exp.B	0.52	0.72	1	3	300	200	7.7×10^{-14}	7.7×10^{-14}	1.8×10^{-14}	0.6×10^{-14}

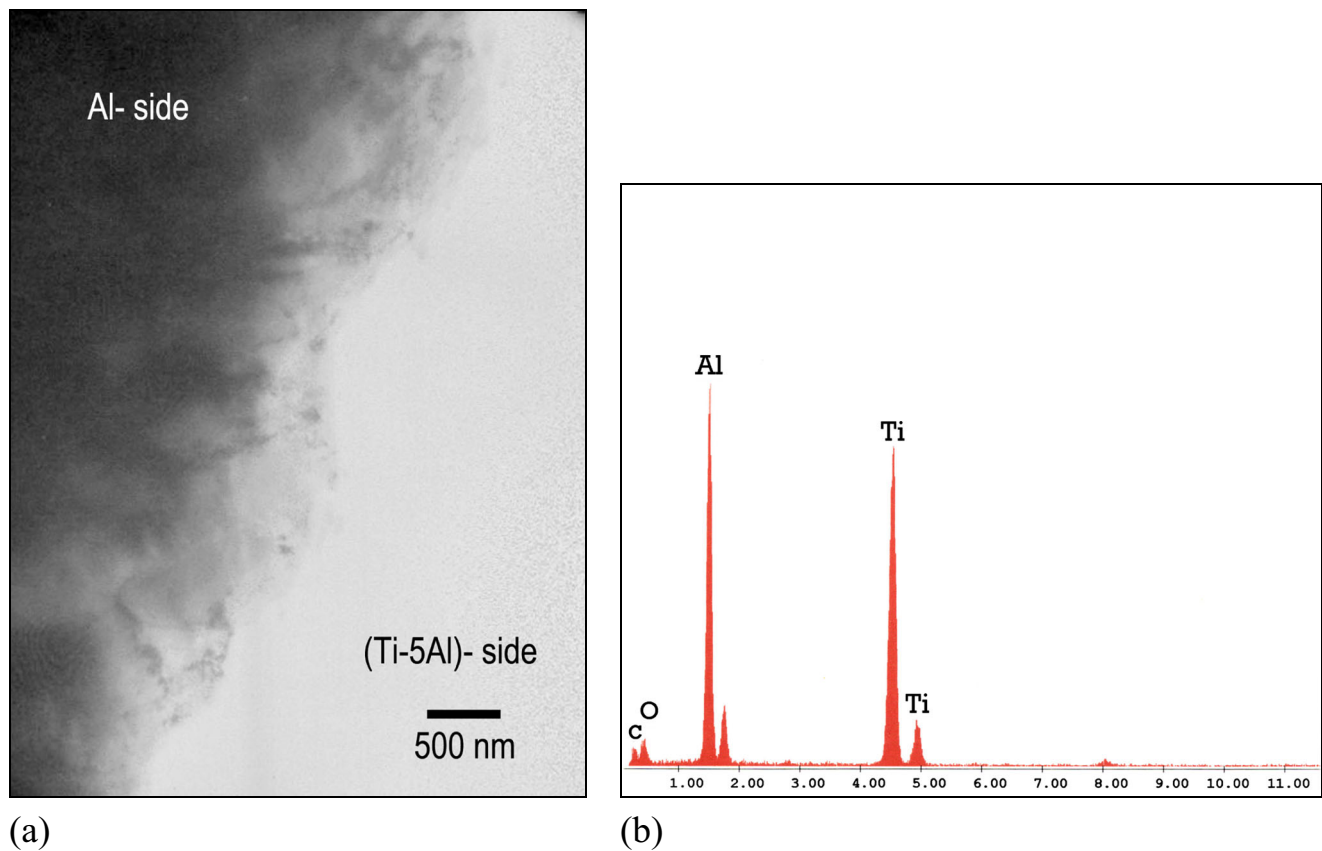


Fig. 7 TEM study at the Ti/Al interface after diffusion welding: (a) TEM image at the interface, (b) EDX at the interface in the Al side (Ti = 44 at. %, Al = 52.4 at. %, O \approx 3.6 at. %)

by applying pressure on the welded sample. This led to the break-up of the protective Al oxide film into small pieces, which allowed the diffusion processes to occur at the Ti alloy/Al interface.

- Two different diffusion systems, (α -Ti)/Al welded at 610 °C for 1 h and ($\alpha + \beta$) Ti/Al joined at 630 °C for 3 h were studied. The diffusion welding was indicated visually as well as by analyses with light, SEM, TEM microscopy and by impact testing of the welded samples.
- EDX analyses at positions near the interface showed Al diffusion into Ti alloy and Ti diffusion into Al. The formation of Al_3Ti , TiAl , and Ti_3Al intermetallic phases was suggested in diffusion zones.
- Studies of diffusion welding of Ti alloys with Al, under the conditions used, showed that the brittle TiAl_3 intermetallic phase layer is not sufficiently thick to cause interface cracking. It was noted that the welding temperature had the greatest influence on the quality of the welds.
- We consider that further study of the development of diffusion welding regimes in ambient air atmosphere would be appropriate in order to spread the knowledge of this welding process in industry for practical applications

including the manufacturing of Ti/Al composites. The current process is simpler and more economical in comparison with welding under a vacuum.

Acknowledgements The authors thank members of the Materials Science Laboratory at the University of Liverpool for their help and support.

Publisher's note Springer Nature remains neutral with regard to jurisdictional claims in published maps and institutional affiliations.

References

- Majumdar B, Galun R, Wesheit A, Mordike BL (1997) Formation of crack-free joint between Ti alloy and Al by using a high-power CO₂ laser. *J Mater Sci* 32:6191–6200. <https://doi.org/10.1023/A:101862072>
- Oliveira JP, Panton B, Zeng Z, Andrei CM, Zhou Y, Miranda RM, Barz Fernandes FM (2016) Laser joining of NiTi to Ti6Al4V using a niobium interlayer. *Acta Mater* 105:9–15. <https://doi.org/10.1016/j.actamat.2015.12.021>
- ASM Handbook Vol 3 (1992), Alloy phase diagrams. ASM International, Materials Park, Geauga County, p 25–307
- Enjyo T, Ikeuchi K, Kanai M, Maruyama T (1977) Diffusion welding of aluminum to titanium. *Osaka University, Transactions of JWRI* 6(1):123–130

5. Enjyo T, Ikeuchi K, Ando M, Hamada K (1985) Diffusion welding of Al-Cu-Mg series A2017 alloy to titanium. Osaka University, Japan, Transactions of JWRI 14(2):293–297
6. Luo J-G, Acoff VL (2000) Interfacial reactions of titanium and aluminum during diffusion welding. *Weld J* 79(9):239–243-s
7. Xu L, Cui YY, Hao YL, Yang R (2006) Growth of intermetallic layer in multi-laminated Ti/Al diffusion couples. *J Mater Sci Eng A* 435–436:638–647. <https://doi.org/10.1016/j.msea.2006.07.077>
8. Wei Y, Wu A, Guisheng Z, Jialie R (2008) Formation process of the bonding joint in Ti/Al diffusion bonding. *J Mater Sci Eng A* 480(1–2):456–463. <https://doi.org/10.1016/j.msea.200707027>
9. Yeh MS, Tseng YH, Chluang TH (1999) Effect of superplastic deformation on diffusion welding of SuperDux 65 stainless steel. *Weld J* 78(9):301–304-s
10. Karfoul MK, Tatlock GJ, Murray RT (2007) The behaviour of Fe and Al at the interface during carbon steel diffusion to aluminium. *J Mater Sci* 42(14):5692–5699. <https://doi.org/10.1007/s10853-006-0742-z>
11. Bondar AV, Peshkov VV, Kireev LS, Shuroupov VV (1998) Diffuzionnaia Svarka Titana i ego Splavov. Voronezh University, Russia, p 160
12. Seith W (1995) Diffusion in Metallen. Springer-Verlag, Berlin, pp 157–180. <https://doi.org/10.1002/ange.19520641402>
13. Reed-Hill R (1973) Physical metallurgy principles. In: Van D (ed) Technology & Engineering, 2nd edn. Van Nostrand, New York, p 378–430
14. Schutze M (1995) Mechanical properties of oxide scales. *Oxid Met* 44(1–2):29–61. <https://doi.org/10.1007/BF01046722>
15. Evans AG, Crumley GR, Demarey (1983) On the mechanical behaviour of brittle coating and layers. *Oxid Met* 20(5–6):193–216. <https://doi.org/10.1007/BF00656841>
16. Robertson J, Manning MI (1990) Limits to the adherence of oxide scales. *Mater Sci Technol* 6(1):81–91. <https://doi.org/10.1179/mst.1990.6.1.81>
17. Benard J (1962) L'Oxidation Des Metaux. Vol.2 (1968) Gauthier Villars, Paris, Russian Translation, Metallurgia, Moscow, pp 312–320
18. Rosa CJ (1970) Oxygen Diffusion in alpha and beta titanium in the temperature range 932° to 1142°C. *Metall Mater Trans B* 1(9): 2517–2522. <https://doi.org/10.1007/BF03038377>
19. Nakajima H, Masahiro K (1991) Diffusion in titanium. *ISIJ International* 31(8):757–766. <https://doi.org/10.2355/isijinternational.31.757>